Density Functional Theory Investigation of Bis(Benzimidazole) Silver (I) Nitrate

Rumyana Yankova, Lachezar Radev

International Journal of Engineering and Information Systems (IJEAIS)
ISSN: 2000-000X
Vol. 1 Issue 6, August – 2017, Pages: 162-171

Density Functional Theory Investigation of Bis(Benzimidazole) Silver (I) Nitrate

Rumyana Yankova[1], Lachezar Radev[2]
[1]Department of Inorganic and Analytical Chemistry, Assen Zlatarov University, 8010 Burgas, Bulgaria,
r_iankova@yahoo.com
[2]Department of Fundamental Chemical Technology, University of Chemical Technology and Metallurgy, 1756 Sofia, Bulgaria,
l_radev@abv.bg

***Abstract*:** *The geometry, chemical reactivity and electronic structure of a bis(benzimidazole)silver (I) nitrate ($[Ag(benzimidazole)_2]^+[NO_3]^-$) were discussed on the basis of Density Functional Theory calculations using B3LYP/6-31G(d,p) and LANL2DZ for silver atom. The calculations indicated that $[Ag(benzimidazole)_2]^+[NO_3]^-$ exists in the form of an ion pair. A large electropositive potential was found on the benzimidazole ligands, while the regions of a negative electrostatic potential is linked with the lone pair of electronegative oxygen atoms in nitrate anion ($[NO_3]^-$). The natural bond orbital theory was using to describe electron transfer both within the anion, and between the anion and cation of an ion pair. The energy values of –5.1508 and –2.0907 eV were calculated to HOMO and LUMO orbitals, respectively.*

Keywords: bis(benzimidazole)silver (I) nitrate, quantum chemical calculations, geometry optimization, electronic properties

1. INTRODUCTION

Imidazoles and benzimidazoles have far reaching applications in the field of chemistry and beyond [1]. Benzimidazole and its derivatives are known to possess antibacterial, antifungal, antiviral and antiproliferative properties [2,3]. They involved in a great variety of biological processes and are used as a procarcinogenic or mutagenic compound. They contain both the imidazole ring and a larger conjugated π system, capable of acting as hydrogen-bond donors and for π–π stacking interaction. Benzimidazoles have different activities as they can act as bacteriostats or bactericides, anticarcinogens, etc [4,5].

Most of the biological studies on silver (I) complexes are on their antimicrobial activity [6-9]. Lately, however, there has been increasing interest in exploring the anti-tumor properties of silver (I) complexes [10-12]. They have been found to exhibit greater cytotoxic activity than of cisplatin. The combination of benzimidazole derivatives with silver ions leads the production of compounds with properties which can be an alternative to existing treatments [13,14].

To predict properties and design more effective metal complexes with benzimidazole and choose a more suitable one for a specific application, theoretical study at the molecular level seems to be necessary. In our previous works we are reported about geometry, electronic structures and chemical reactivity of many complexes with benzimidazole [15-20]. The use of density functional theory (DFT) makes an important contribution to promotion of theoretical calculations. In this work, a theoretical study on the geometry, electronic structure and chemical reactivity of the bis(benzimidazole)silver (I) nitrate by density functional theory (DFT) calculations using B3LYP method with the 6-31G(d,p) basis set and LANL2DZ for silver atom was carried out.

.

2. EXPERIMENTAL

The complex was obtained by mixing EtOH solutions of the silver nitrate and benzimidazole in molar ratio 1:2. The product which precipitated (after one week) was filtered off, washed with EtOH and dried in vacuum over $CaCl_2$. The identification of [Ag(benzimidazole)2]NO3 was carried out by means of IR spectroscopy. The infra-red spectra were recorded on a Bruker Tensor 27 FT-IR spectrometer in the 4000 – 400 cm–1 range, with the samples embedded in KBr matrixes. Characterization results: 3148.82, 3116.32, 3055.71, 2915.90, 1751.10, 1625.11, 1598.36, 1493.51, 1463.21, 1439.56, 1367.65, 1343.51, 1303.04, 1276.02, 1248.73, 1130.79, 1105.61, 1006.27, 969.85, 820.41, 760.03, 739.92, 727.69, 632.18, 608.17, 429.11, 416.25 cm^{-1}.

3. COMPUTATIONAL METHODS

Computational calculation of $[Ag(benzimidazole)_2]^+[NO_3]^-$ was performed by using Gaussian 03W package [21] and GaussView, Version 6 molecular visualized program [22]. The theoretical calculations were performed using the Density Functional Theory (DFT) [23,24] along with the three-parameter hybrid functional (B3) for the exchange part and the Lee-Yang-Parr (LYP) correlation functional [25-28]. The 6-31G(d,p) and LANL2DZ [29-31] for silver atom were used as a basis set. The DFT hybrid B3LYP functional tend to overestimate the fundamental modes, therefore scaling factor of 0.9613 has to be used for

obtaining a considerably better agreement with experimental data [32]. The frequency calculations were employed to confirm the structure as minimum points in energy. The absence of imaginary wavenumbers on the calculated vibrational spectrum confirms that the structure deduced corresponds to minimum energy.

The Highest Occupied Molecular Orbital (HOMO)-Lowest Unoccupied Molecular Orbital (LUMO) analysis has been carried out to explain the charge transfer place within the molecule. The chemical hardness and chemical potential are also calculated. Molecular Electrostatic Potential (MEP) analysis was obtained from the optimized structure. MEP surface mapping is investigated to comment upon the reactive nature of the title compound. The Natural Bond Orbital (NBO) [33] analysis was carried out utilizing the optimized geometry at DFT/B3LYP level using NBO program [34] under Gaussian 03W program package in order to understand inter- and intra-molecular delocalization or hyperconjugation.

4. RESULTS AND DISCUSSION

4.1. Geometry Optimization

The optimized ground state molecular geometry of bis(benzimidazole)silver (I) nitrate was obtained by B3LYP with 6-31G(d,p) basis set and LANL2DZ for silver atom. The optimized structural parameters were used in the vibrational frequency calculations at the DFT level to characterize the stationary point as minima (convergence criterion 10^{-8} a.u.). The absence of imaginary frequencies in the calculated vibrational spectrum confirms that the structure corresponds to minimum energy. The optimized molecular structure with the numbering of atoms is given in Figure 1. The geometrical parameters (bond lengths and bond angles) corresponding to the optimized geometry of the title molecule are given in Table 1.

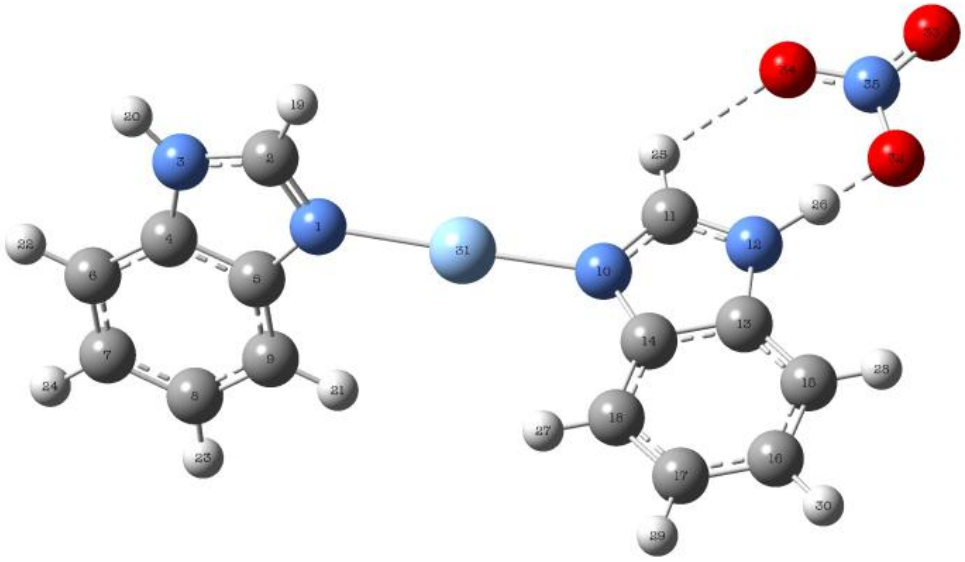

Fig. 1. *Optimized molecular structure and atom numbering of bis(benzimidazole)silver (I) nitrate: O-atoms are in red, Ag-atom is in light blue, N-atoms are in dark blue, C-atoms are in grey, H-atoms are in white.*

The calculated bond lengths and bond angles are in good agreement with XRD of similar compounds. The data showed that the longest distance of 2.165 Å is registered for Ag–N bond in the bis(benzimidazole)silver (I) cation. The typical Ag–N bond lengths are within the range 2.1 – 2.4 Å [35-37]. The N^{35}–O^{33} bond separation exhibits the shortest distance of 1.217 Å, while N^{35}–O^{34} one is the next – 1.225 Å. It was observed that the hydrogen atom (H^{26}) connected with the imidazole ring forms a hydrogen bond to O^{32}. As a consequence the N^{35}–O^{32} bond length is 1.251 Å [38].

It is worth noted that a difference between calculated and experimentally estimated geometrical parameters exists. The observed discrepancy is due to the fact that theoretical calculations were carried out in gas phase, while the experimentally obtained crystal data were conducted in condense phase.

Table 1: Some optimized geometrical parameters of bis(benzimidazole)silver (I) nitrate

Structural parameters		
	B3LYP 6-31G(d,p)	**X-ray data**
Bond length (Å)		
$Ag^{31}–N^{1}$	2.149	2.165 [39]; 2.149 [40]
$Ag^{31}–N^{10}$	2.090	2.165 [39]; 2.180 [40]
$N^{1}–C^{2}$	1.320	1.32 [41]
$N^{10}–C^{11}$	1.344	1.33 [41]
$C^{2}–N^{3}$	1.357	1.35 [41]
$C^{11}–N^{12}$	1.333	1.35 [41]
$N^{3}–C^{4}$	1.389	1.36 [41]
$N^{12}–C^{13}$	1.383	1.37 [41]
$C^{4}–C^{5}$	1.410	1.40 [41]
$C^{13}–C^{14}$	1.415	1.40 [41]
$C^{5}–N^{1}$	1.396	1.38 [41]
$C^{14}–N^{10}$	1.392	1.40 [41]
$C^{4}–C^{6}$	1.397	1.39 [41]
$C^{13}–C^{15}$	1.399	1.40 [41]
$C^{6}–C^{7}$	1.391	1.36 [41]
$C^{15}–C^{16}$	1.391	1.37 [41]
$C^{7}–C^{8}$	1.411	1.41 [41]
$C^{16}–C^{17}$	1.411	1.40 [41]
$C^{8}–C^{9}$	1.389	1.37 [41]
$C^{17}–C^{18}$	1.391	1.39 [41]
$C^{9}–C^{5}$	1.399	1.39 [41]
$C^{18}–C^{14}$	1.399	1.38 [41]
$N^{12}–H^{26}$	1.162	0.94 [38]
$H^{26}\cdots O^{32}$	1.355	1.86 [38]
$H^{25}\cdots O^{34}$	2.330	2.78 [38]
$O^{32}–N^{35}$	1.306	1.251 [38]
$O^{33}–N^{35}$	1.229	1.217 [38]
$O^{34}–N^{35}$	1.253	1.225 [38]
Valence angle (degree)		
$N^{1}–Ag^{31}–N^{10}$	179.0	180.0 [39]
$Ag^{31}–N^{1}–C^{5}$	127.0	128.0 [41]; 126.9 [39]
$Ag^{31}–N^{10}–C^{14}$	128.9	127.9 [41]
$Ag^{31}–N^{1}–C^{2}$	126.8	125.0 [41];127.0 [39]
$Ag^{31}–N^{10}–C^{11}$	125.6	126.0 [41]
$N^{1}–C^{2}–N^{3}$	112.1	111.6 [41]
$N^{10}–C^{11}–N^{12}$	113.4	112.3 [41]
$C^{2}–N^{3}–C^{4}$	107.9	108.8 [41]
$C^{11}–N^{12}–C^{13}$	106.6	107.4 [41]
$N^{3}–C^{4}–C^{5}$	105.0	104.7 [41]
$N^{12}–C^{13}–C^{14}$	106.9	106.7 [41]
$C^{4}–C^{5}–N^{1}$	108.9	109.5 [41]
$C^{13}–C^{14}–N^{10}$	107.6	107.8 [41]
$C^{5}–N^{1}–C^{2}$	106.2	105.5 [41]
$C^{14}–N^{10}–C^{11}$	105.4	105.8 [41]
$C^{4}–C^{6}–C^{7}$	116.5	117.6 [41]
$C^{13}–C^{15}–C^{16}$	117.2	116.2 [41]
$C^{6}–C^{7}–C^{8}$	121.7	121.2 [41]
$C^{15}–C^{16}–C^{17}$	121.5	121.8 [41]
$C^{7}–C^{8}–C^{9}$	121.6	121.3 [41]
$C^{16}–C^{17}–C^{18}$	121.4	121.6 [41]
$C^{8}–C^{9}–C^{5}$	117.4	118.5 [41]

$C^{17}–C^{18}–C^{14}$	117.6	117.4 [41]
$C^{9}–C^{5}–C^{4}$	120.5	119.5 [41]
$C^{18}–C^{14}–C^{13}$	120.8	120.6 [41]
$C^{5}–C^{4}–C^{6}$	122.4	121.9 [41]
$C^{14}–C^{13}–C^{15}$	121.4	122.4 [41]
$N^{3}–C^{4}–C^{6}$	132.6	133.4 [41]
$N^{12}–C^{13}–C^{15}$	131.6	130.9 [41]
$N^{1}–C^{5}–C^{9}$	130.6	130.9 [41]
$N^{10}–C^{14}–C^{18}$	131.5	131.6 [41]
$C^{11}–N^{12}–H^{26}$	122.7	119.0 [38]
$N^{12}–H^{26}\cdots O^{32}$	179.7	171.0 [38]
$O^{32}–N^{35}–O^{34}$	118.4	118.4 [38]
$O^{34}–N^{35}–O^{33}$	123.2	122.1 [38]
$O^{33}–N^{35}–O^{32}$	118.5	119.5 [38]
Dihedral angle (degree)		
$C^{2}–N^{1}–N^{10}–C^{11}$	–65.3	–
$C^{5}–N^{1}–N^{10}–C^{14}$	–69.3	–
$C^{11}–N^{12}–O^{32}–N^{35}$	1.4	–
$C^{15}–C^{13}–N^{12}–O^{32}$	–0.96	–

4.2. Homo-Lumo Analysis

It is well known that in quantum chemistry there are two of the most important parameters − highest occupied molecular orbital (HOMO) and lowest unoccupied molecular orbital (LUMO). They allow the investigation of stability and reactivity of the molecules [42]. The HOMO represents the ability to donate an electron, while the LUMO represents the ability to accept an electron [43]. The larger values of the energy difference will provide low reactivity to a chemical species. The lower values of the energy difference will render good inhibition efficiency, because the energy to remove an electron from the last occupied orbital will be low. The energies of frontier molecular orbitals and their orbital energy gap were calculated using B3LYP/6-31G(d,p) level and LANL2DZ for silver atom. The 3D plots generated from the calculations are illustrated in Figure 2. Results showed that HOMO is delocalized on the nitrate anion (Figure 2(1)) includes mainly the *p*-orbitals of the oxygen atoms as the contribution – ψ_{HOMO} = 19.6% $2p_y(O^{34})$ – 12.7% $2p_x(O^{33})$ + 12.7% $2p_x(O^{32})$ – 12.1% $2p_y(O^{33})$ + 9.8% $3p_y(O^{34})$ – 7.0% $3p_x(O^{33})$. Unlike HOMO, LUMO is delocalized on the benzimidazole ring (Figure 2(2)) involves the *p*-orbitals of the carbon atoms as the contribution – ψ_{LUMO} = 13.3% $3p_y(C^{2})$ + 10.7% $2p_y(C^{2})$ + 7.3% $3p_y(C^{9})$ + 6.9% $3p_y(C^{6})$ + 5.4% $2p_y(C^{9})$ + 4.8% $2p_y(C^{6})$.

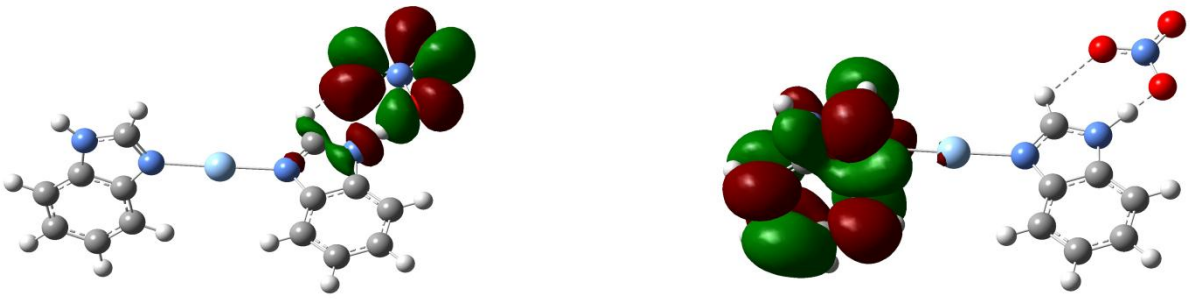

1 2

Fig. 2. *Frontier molecular orbitals of bis(benzimidazole)silver (I) nitrate: HOMO (1) and LUMO (2)*

The energy of HOMO and LUMO orbitals are related to the ionization potential (*I*) and electron affinities (*A*) [44]: $I = -E_{HOMO}$ = 5.1508 eV; $A = -E_{LUMO}$ = 2.0907 eV; $\Delta E_{LUMO–HOMO}$ = 3.0601 eV. Using HOMO and LUMO energy values [45] and approximations of Koopman's theorem [46], the global quantum molecular descriptors such as global (chemical) hardness (η) and softness (σ), electronegativity (χ), chemical potential (μ) and electrophilicity index (ω) were calculated. The hardness and softness were suggested in literature to denote resistance to deformation by mechanical force [47]. The mathematical expression of (η) and (σ) can be written as:

$$\eta = \frac{1}{2}\left(E_{LUMO} - E_{HOMO}\right) \quad (1)$$

$$\sigma = \frac{1}{2\eta} \quad (2)$$

The global hardness (η) and softness (σ) for the bis(benzimidazole)silver (I) nitrate are 1.53005 and 0.3268 eV, respectively.

Electronegativity is the tendency of molecules to attract electrons [48]. Parr and Yang attempted to quantify this descriptor [49]. This is found by the average of HOMO and LUMO energy values:

$$\chi = -\frac{1}{2}\left(E_{HOMO} + E_{LUMO}\right) \quad (3)$$

The electronegativity is a measure of resistance of an atom or ion, or a group or atoms in a molecule for an entering electronic charge. The electronegativity of our compound is 3.6208 eV.

Chemical potential denotes the affinity of an electron to escape and is defined as the first derivative of the total energy with respect to the number of electrons in a molecule [50]. The chemical potential is simply the negative of electronegativity value. It is given as:

$$\mu = -\chi = \frac{1}{2}\left(E_{HOMO} + E_{LUMO}\right) \quad (4)$$

The chemical potential of the bis (benzimidazole) silver (I) nitrate is –3.6208 eV.

The capability of a substance to accept electrons is quantified as electrophilicity index (ω). Parr et al. defined the electron affinity as the capability of a substance to have only one electron from the surroundings [47]. This index measures the energy lowering of a substance due to the electron flow between donor and acceptor. Parr and co-workers [50] suggested that ω can be measured through the equation:

$$\omega = \frac{\mu^2}{2\eta} \quad (5)$$

The electrophilicity index for our compound is 4.2841 eV.

4.3. Molecular Electrostatic Potentials and Atomic Charges

Atomic charges affect molecular properties such as dipole moment, polarizability and electronic structure. The net charge, which is localized in the respective atom, is result of the redistribution of the electrons in the molecule. The calculated charge distribution by Mulliken population analysis [51] and Natural population analzsis (NPA charges) [52] for the title compound is presented in Figure 3. The result shows that the positive charges are mainly localized on nitrogen atom in nitrate anion, silver atom and hydrogen atoms, while the carbon atoms are found to be either positive or negative. The nitrogen atoms in imidazole ring and oxygen atoms in nitrate anion are found to be negative.

Molecular Electrostatic Potential (MEP) is used to predict the relative sites for nucleophilic or electrophilic attack and to predict macroscopic properties [53, 54]. The 3D plot of the molecular electrostatic potential was calculated by using the optimized molecular structures at B3LYP/6-31G(d,p) level and LANL2DZ for silver atom for the bis(benzimidazole)silver (I) nitrate. It was established that the value of molecular electrostatic potential undergoes alteration form –0.09888 to +0.10567 a.u. The results are illustrated in Figure 4. The electrostatic potential at the surface is presented by different colors: red – regions of negative, blue – regions of positive and green – zero electrostatic potential. The negative regions of MEP are related to electrophilic reactivity, and the positive regions are related to the nucleophilic reactivity. As can be seen from Figure 4, the negative electrostatic potential is localized over the oxygen atoms of the nitrate anion, and is potential site for electrophilic attach. The positive regions are localized around the complex cation.

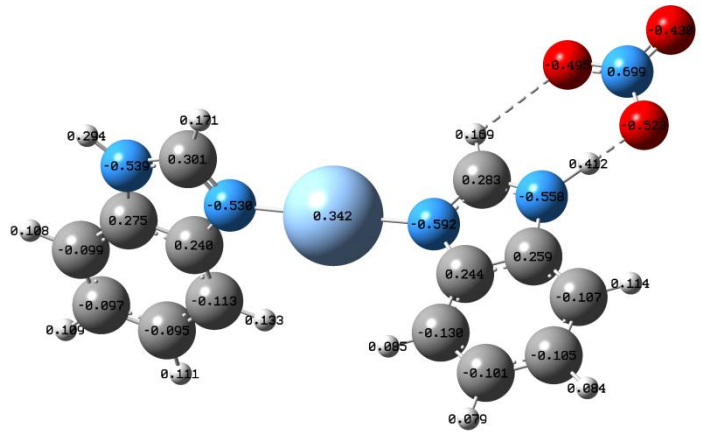

1

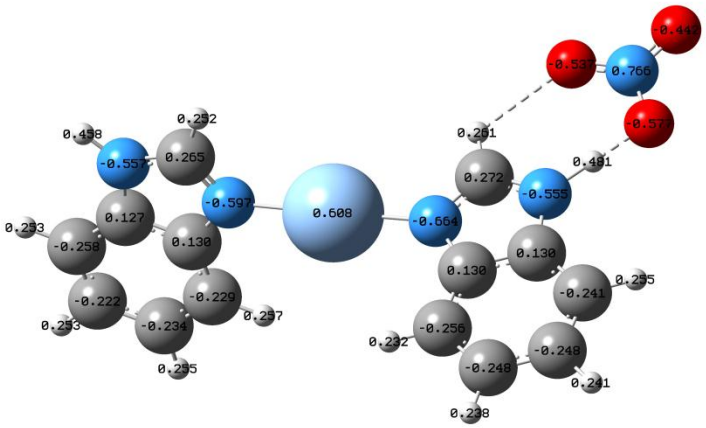

2

Fig. 3. *Mulliken atomic charges (**1**) and NPA atomic charges (**2**) for bis(benzimidazole)silver (I) nitrate*

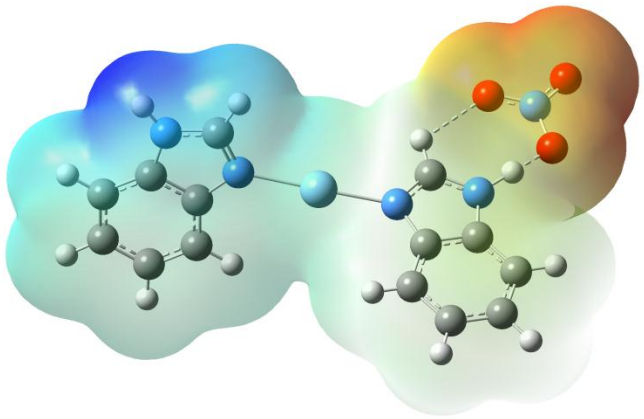

Fig. 4. *Molecular electrostatic potential surface for bis(benzimidazole)silver (I) nitrate*

4.4. Natural Bond Orbital (NBO) Analysis

The donor-acceptor interactions and main charge distribution between the anion and cation in ion pair $[Ag(benzimidazole)_2]^+[NO_3]^-$ and nature of coordinate bonds were investigated using natural bond orbital analysis [52]. The intensity of the donor-acceptor interactions was denoted by second order stabilization energy $E(2)$. The stabilization energy value inversely dependents on the difference between the energies of particular acceptor and donor orbitals. The latter can be written by expression:

$$E(2) = -n_\sigma \frac{\left\langle \sigma_i | F | \sigma_j \right\rangle^2}{E_j - E_i} = -n_\sigma \frac{F_{ij}^2}{\Delta E} \quad (6)$$

where, $E(2)$ is energy of stabilization (kcal/mol), n_σ is population donor orbital, F_{ix}^2 are Fok's matrix elements and ΔE is difference between the energies of acceptor and donor orbitals (kcal/mol). Donor-acceptor interactions between nonbonding-antibonding, bonding-antibonding and antibonding-antibonding orbitals decrease population of occupied orbital and electron density transmission towards antibonding orbital. The stronger of the donor-acceptor capacity will be as the larger of $E(2)$ value is. Only interesting donor-acceptor interactions and their second order stabilization energies in $[Ag(benzimidazole)_2]^+[NO_3]^-$ are presented in Table 2.

Table 2. Some donor-acceptor interactions and their second order stabilization energies in $[Ag(benzimidazole)_2]^+[NO_3]^-$, calculated from NBO analysis by B3LYP/6–31G(d,p) method

Donor (*i*)	ED (*i*)/	Acceptor (*x*)	ED (*x*)/e	E(2)	E(*x*) – E(*i*)	F(*i*,*x*).
	(e)	(e)		(kcal/mol)	(a.u.)	(a.u)
LP(1) N^1	1.801	LP(6)* Ag^{31}	0.371	53.01	0.42	0.139
LP(1) N^{10}	1.747	LP(6)* Ag^{31}	0.371	74.09	0.37	0.153
LP(1) O^{32}	1.970	$\sigma^* N^{12}$–H^{26}	0.192	10.23	0.97	0.093
LP(2) O^{32}	1.786	$\sigma^* N^{12}$–H^{26}	0.192	102.38	0.78	0.254
LP(2) O^{33}	1.887	$\sigma^* O^{32}$–N^{35}	0.109	21.18	0.57	0.098
LP(2) O^{33}	1.887	$\sigma^* O^{34}$–N^{35}	0.075	18.01	0.67	0.099
LP(2) O^{34}	1.901	$\sigma^* O^{32}$–N^{35}	0.109	16.65	0.58	0.088
LP(2) O^{34}	1.901	$\pi^* O^{33}$–N^{35}	0.060	16.23	0.73	0.098
$\sigma^* O^{32}$–N^{35}	0.109	$\sigma^* N^{12}$–H^{26}	0.192	11.55	0.02	0.038

E(2) – stabilization energy, kcal/mol
ED (i) – occupied donor orbital
ED (*x*) – occupied acceptor orbital
E(*x*) – *E* (*i*) – difference between the energies of acceptor and donor orbital, a.u.
F(*i*, *x*) – Fok's matrix elements, a.u.

The obtained results showed that interactions between nonbonding donor orbitals form nitrogen atoms (LP(1)N^1, LP(1)N^{10}) and antibonding LP(6)* of silver atom increases ED(0.371e) that weakens the respective nonbonding orbitals ED(1.801, 1.747e) leading to stabilization of 53.01 and 74.09 kcal/mol, respectively. Therefore, the bonds N–Ag are formed due to charge transfer from nitrogen atoms to silver atom. The Mayer bond orders for these two coordinate bonds are 0.449 and 0.576. It was observed strong donor-acceptor interaction between LP(1), LP(2) O^{32} with $\sigma^* N^{12}$–H^{26} which decreases the population of occupied orbitals (1.970, 1.786e) and increases the population of acceptor antibonding orbital (0.192e). As a result, stabilization energy values of 10.23 and 102.38 kcal/mol were obtained. The latter is a consequence of the charge transfer from oxygen atom to hydrogen one. As a part of the stabilization energy of intramolecular interacting system, charge transfer plays a crucial role during the hydrogen bonds formation [55, 56].

Calculated electron density contours with hydrogen bond critical point using B3LYP/6-311+G(d,p) are presented in Figure 5.

The hydrogen bond critical point is a specific point between the donor and acceptor, where the gradient of electron density is zero, and it is essential evidence of hydrogen bond existence [56-60]. Here it is observed that intramolecular hydrogen bond distance ($O^{32}\cdots H^{26}$) is 1.355 Å and Mayer bond order of 0.300. In addition, significantly weaker hydrogen bond between O^{34} and H^{25} was observed. The latter was expressed by bond length and bond order values of 2.330 Å and 0.030, respectively.

From NBO atomic charges shown in Figure 4 confirm the results obtained by means of FMO analysis that most of the negative charge is located on O^{32} (–0.577) and O^{34} (–0.537) atoms in the anion $[NO_3]^-$. Based on the calculated bond order values in $[Ag(benzimidazole)_2]^+[NO_3]^-$ it could be assumed that N^1–Ag^{31} (0.449), N^{10}–Ag^{31} (0.576) bonds are significantly higher than the order (0.300) of $O^{32}\cdots H^{26}$ bond. The obtained results suggest that the $O^{32}\cdots H^{26}$–N^{12} bond seems to be the most reactive area in the synthesized $[Ag(benzimidazole)_2]^+[NO_3]^-$. The bond lengths for bonds with H atoms are not well measured by X-ray diffraction.

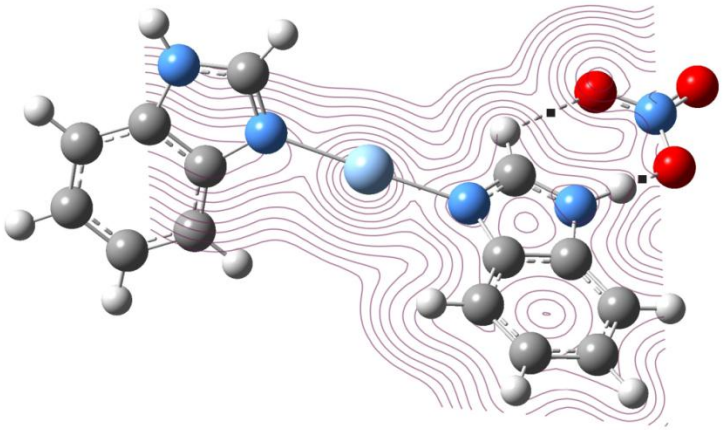

Fig. 5. *Contour map of the electron density for bis(benzimidazole)silver (I) nitrate. Hydrogen bond critical point is indicated by filled square symbol (■).*

5. CONCLUSION

The bis(benzimidazole) silver (I) nitrate ($[Ag(benzimidazole)_2]^+[NO_3]^-$) was synthesized. The complete molecular structural parameters, electronic structure and chemical reactivity were optimized with DFT-B3LYP methods using 6-31G(d,p) basis sets and LANL2DZ for silver atom. Quantum chemical descriptors such as global hardness and softness, chemical potential, electronegativity and electrophilicity index, HOMO–LUMO energy gap and HOMO/LUMO energy were studied. Molecular electrostatic potential analysis showed that the most negative charge is localized around the nitrate anion ($[NO_3]^-$), while a large electropositive potential is observed in the area of complex cation ($[Ag(benzimidazole)_2]^+$. The NBO analysis indicated the intramolecular charge transfer between the bonding and antibonding orbitals. Mullikan and natural charge distribution of the $[Ag(benzimidazole)_2]^+[NO_3]^-$ were studied which indicated the electronic charge distribution in the molecule.

6. REFERENCES

[1] R.T. Stibrany. Rutgers The State University of New Jersey-New Brunswick, 2008.

[2] Y. Bansal, O. Silakari, The therapeutic journey of benzimidazoles: a review, Bioorganic & medicinal chemistry, 20 (2012) 6208–6236.

[3] V.A. Sontakke, A.N. Kate, S. Ghosh, P. More, R. Gonnade, N.M. Kumbhar, V.S. Shinde, Synthesis, DNA interaction and anticancer activity of 2-anthryl substituted benzimidazole derivatives, New Journal of Chemistry, 39 (2015) 4882–4890.

[4] H. Küçükbay, R. Durmaz, E. Orhan, S. Günal, Synthesis, antibacterial and antifungal activities of electron-rich olefins derived benzimidazole compounds, Il Farmaco, 58 (2003) 431–437.

[5] L. Garuti, M. Roberti, C. Cermelli, Synthesis and antiviral activity of some N-benzenesulphonylbenzimidazoles, Bioorganic & medicinal chemistry letters, 9 (1999) 2525–2530.

[6] N. Farrell, Metal complexes as drugs and chemotherapeutic agents, Comp. Coord. Chem. II, 9 (2003) 809–840.

[7] A. Melaiye, W.J. Youngs, Silver and its application as an antimicrobial agent, 2005.

[8] S. Silver, Le T., Phung, G. Silver, Silver as biocides in burn and wound dressings and bacterial resistance to silver compounds, Journal of Industrial Microbiology and Biotechnology, 33 (2006) 627–634.

[9] A. Lansdown, Silver in healthcare: its antimicrobial efficacy and safety in use, Royal Society of Chemistry, 2010.

[10] T.N. Wells, P. Scully, G. Paravicini, A.E. Proudfoot, M.A. Payton. Mechanism of irreversible inactivation of phosphomannose isomerases by silver ions and flamazine, Biochemistry, 34 (1995) 7896–7903.

[11] K. Nomiya, K. Tsuda, T. Sudoh, M. Oda, Ag (I) N bond-containing compound showing wide spectra in effective antimicrobial activities: Polymeric silver (I) imidazolate, J. Inorg. Biochem., 68 (1997) 39–44.

[12] I. Tsyba, B.K. Mui, R. Bau, R. Noguchi, K. Nomiya, Synthesis and structure of a water-soluble hexanuclear silver (I) nicotinate cluster comprised of a "cyclohexane-chair"-type of framework, showing effective antibacterial and antifungal activities: Use of "sparse matrix" techniques for growing crystals of water-soluble inorganic complexes, Inorg. Chem., 42 (2003) 8028–8032.

[13] M. McCann, R. Curran, M. Ben-Shoshan, V. McKee, M. Devereux, K. Kavanagh, A. Kellett, Synthesis, structure and biological activity of silver (I) complexes of substituted imidazoles, Polyhedron, 56 (2013) 180–188.

[14] R.A. Haque, P.O. Asekunowo, M.R. Razali, Dinuclear silver (I)-N-heterocyclic carbene complexes of N-allyl substituted (benz) imidazol-2-ylidenes with pyridine spacers: synthesis, crystal structures, nuclease and antibacterial studies, Transition Metal Chemistry, 39 (2014) 281–290.

[15] R. Yankova, L. Radev, Structural and Electronic Properties of [Co(benzimidazo-le)$_2$I$_2$], International Journal of Materials and Chemistry, 6 (2016**)** 19–27.

[16] R. Yankova, Natural Bond Population Analysis of dichlorobis(benzimidazo-le)Co(II) complex, Physical Chemistry: An Indian Journal, 11 (2016) 1–6.

[17] R. Yankova, Study on dibromo-bis(benzimidazole)Co(II) complex. I. Molecular structure and vibrational analysis, Industrial Thechnologies, 3 (2016) 146–150.

[18] R. Yankova, Study on dibromo-bis(benzimidazole)Co(II) complex. II. Natural bond orbital (NBO) analysis, Industrial Thechnologies, 3 (2016) 151–154.

[19] R. Yankova, Structural and electronic properties of [Cd(benzimidazole)$_2$Cl$_2$], Science & Technologies, 6 (2016) 63–70.

[20] R. Yankova, L. Radev, St. Avramov, Density functional theory study on the copper(II) complex of benzimidazole, Journal of Multidisciplinary Engineering Science Studies, 4 (2017) 2569–2575.

[21] M.J. Frisch, G.W. Trucks, H.B. Schlegel, G.E. Scuseria, M.A. Robb, J.R. Cheeseman, J.A. Montgomery, T. Vreven, K.N. Kudin, J.C. Burant, J.M. Millam, S.S. Iyengar, J. Tomasi, V. Barone, B. Mennucci, M. Cossi, G. Scalmani, N. Rega, G.A. Petersson, H. Nakatsuji, M. Hada, M. Ehara, K. Toyota, R. Fukuda, J. Hasegawa, M. Ishida, T. Nakajima, Y. Honda, O. Kitao, H. Nakai, M. Klene, X. Li, J.E. Knox, H.P. Hratchian, J.B. Cross, V. Bakken, C. Adamo, J. Jaramillo, R. Gomperts, R.E. Stratmann, O. Yazyev, A.J. Austin, R. Cammi, C. Pomelli, J.W. Ochterski, P.Y. Ayala, K. Morokuma, G.A. Voth, P. Salvador, J.J. Dannenberg, V.G. Zakrzewski, S. Dapprich, A.D. Daniels, M.C. Strain, O. Farkas, D.K. Malick, A.D. Rabuck, K. Raghavachari, J.B. Foresman, J.V. Ortiz, Q. Cui, A.G. Baboul, S. Clifford, J. Cioslowski, B.B. Stefanov, G. Liu, A. Liashenko, P. Piskorz, I. Komaromi, R.L. Martin, D.J. Fox, T. Keith, M.A. Al-Laham, C.Y. Peng, A. Nanayakkara, M. Challacombe, P.M.W. Gill, B. Johnson, W. Chen, M.W. Wong, C. Gonzalez, J.A. Pople, Gaussian 03, Revision B.04, Gaussian, Inc., Wallingford CT, 2004.

[22] GaussView, Version 6, Roy Dennington, Todd A. Keith, and John M. Millam, Semichem Inc., Shawnee Mission, KS, 2016.

[23] P. Hohenberg, W. Kohn, Inhomogeneous electron gas, Phys. Rev. B, 136 (1964) B864.

[24] W. Kohn, L. Sham, Self-consistent equations including exchange and correlation effects, Phys. Rev. A, 140 (1965) A1133.

[25] C.T. Lee, W.T. Yang, R.G. Parr, Development of the Colle-Salvetti correlation-energy formula into a functional of the electron density, Phys. Rev., B 37 (1988) 785–789.

[26] A.D. Becke, Densityfunctional thermochemistry. III. The role of exact exchange, J. Chem. Phys., 98 (1993) 5648–5652.

[27] R.G. Parr, W. Yang, Density-functional theory of atoms and molecules (Vol. 16), Oxford university press, 1989.

[28] P.J. Stephens, F.J. Devlin, C.F. Chabalowski, M.J. Frisch, Ab initio calculation of vibrational absorption and circular dichroism spectra using density functional force fields, J. Phys. Chem., 98 (1994) 11623–11627.

[29] P.J. Hay, W.R. Wadt, Ab initio effective core potentials for molecular calculations. Potentials for the transition metal atoms Sc to Hg, J. Chem. Phys., 82 (1985) 270–283.

[30] W.R. Wadt, P.J. Hay, Ab initio effective core potentials for molecular calculations. Potentials for main group elements Na to Bi, J. Chem. Phys., 82 (1985) 284–298.

[31] P.J. Hay, W.R. Wadt, Ab initio effective core potentials for molecular calculations. Potentials for K to Au including the outermost core orbitals, J. Chem. Phys., 82 (1985) 299–310.

[32] J.B. Forsman, E. Frisch (Ed.). Exploring Chemistry with Electronic Structure Methods: A Guide to Using Gaussian, Gaussian Inc., Pittsburg, PA, 1996.

[33] A.E. Reed, L.A. Curtiss, F. Weinhold, Intermolecular interactions from a natural bond orbital, donor-acceptor viewpoint, Chemical Reviews, 88 (1988) 899–926.

[34] E.D. Gledening, A.E. Reed, J.A. Carpenter, F. Weinhold, NBO. version 3.1.

[35] J.L. Gulbransen, C.M. Fitchett, Anion directed control of supramolecular structure in silver complexes through weak interactions, CrystEngComm, 14 (2012) 5394–5397.

[36] C. Pettinari, F. Marchetti, S. Orbisaglia, R. Pettinari, J. Ngoune, M. Gomez, C. Santos, E. Alvarez, Group 11 complexes with the bidentate di (1 H-indazol-1-yl) methane and di (2H-indazol-2-yl) methane) ligands, CrystEngComm, 15 (2013) 3892–3907.

[37] Q. Sun, Y. Bai, G. He, C. Duan, Z. Lin, Q. Meng, Spontaneous resolution of silver double helicates consisting of achiral ligands with several aromatic rings, Chem. Commun, (2006) 2777–2779.

[38] A.S. Batsanov, Pyridinium nitrate at 290 K, Acta Crystallogr. E Structure Reports Online, 60 (2004) o2424– o2425.

[39] Y. Kim, S.K. Kang, Crystal structure of bis [2-(1H-benzimidazol-2-yl) aniline] silver (I) nitrate Acta Crystallogr. E Crystallogr. Commun., 71 (2015) 1058–1060.

[40] U. Kalinowska-Lis, A. Felczak, L. Chęcińska, I. Szabłowska-Gadomska, E. Patyna, M. Małecki, J. Ochocki, Antibacterial Activity and Cytotoxicity of Silver (I) Complexes of Pyridine and (Benz) Imidazole Derivatives. X-ray Crystal Structure of [Ag (2, 6-di (CH2OH) py) 2] NO3, Molecules, 21 (2016) 87.

[41] M. Bukowska-Strzyżewska, A. Tosik, Crystal and molecular structure of dibromobis (benzimidazole) copper (II), Journal of Chemical Crystallography, 18 (1988) 525–531.

[42] S. Gunasekaran, R.A. Balaji, S. Kumeresan, G. Anand, S. Srinivasan, Experimental and theoretical investigations of spectroscopic properties of N-acetyl-5-methoxytryptamine, Can. J. Anal. Sci. Spectrosc. 53 (2008) 149–160.

[43] S.A. Halim, M.A. Ibrahim, Synthesis, DFT calculations, electronic structure, electronic absorption spectra, natural bond orbital (NBO) and nonlinear optical (NLO) analysis of the novel 5-methyl-8*H*-benzo[*h*]chromeno[2,3-*b*][1,6] naphthyridine-6(5*H*),8-dione (MBCND), J. Mol. Str. 1130 (2017) 543–558.

[44] K. Wolinski, J.F. Hinton, P. Pulay, Efficient implementation of the gauge-independent atomic orbital method for NMR chemical shift calculations, J. Am. Chem. Soc. 112 (23) (1990) 8251–8260.

[45] T. Koopman, Über die Zuordnung von Wellenfunktionen und Eigenwerten zu den Einzelnen Elektronen Eines Atoms, Physica 1 (1–6) (1934) 104–113.

[46] R.G. Pearson, Hard and soft acids and bases, J. Am. Chem. Soc. 85 (22) (1963) 3533–3539.

[47] R.G. Pearson, Absolute electronegativity and hardness correlated with molecular orbital theory, Proc. Natl. Acad. Sci. U.S.A. 83 (1986) 8440–8441.

[48] R.G. Parr, W. Yang, Density-Functional Theory of Atoms and Molecules, Oxford University Press, New York, 1989.

[49] E. Kavitha, N. Sundaranganesan, S. Sebastian, Molecular structure, vibrational spectroscopic and HOMO, LUMO studies of 4-nitroaniline by density functional method, Indian J. Pure Appl. Phys. 48 (1) (2010) 20–30.

[50] R.G. Parr, L.V. Szentpály, S. Liu, Electrophilicity Index, J. Am. Chem. Soc. 121 (9) (1999) 1922–1924.

[51] R.S. Mulliken, Electronic population analysis on LCAO-MO molecular wave functions, J. Chem. Phys. 23 (10) (1955) 1833–1840.

[52] F. Weinhold, C.R. Landis, Natural bond orbitals and extensions of localized bonding concepts, Chem. Educ. Res. Pract. 2 (2001) 91–104.

[53] J.S. Murray, K. Sen, Molecular Electrostatic Potentials, Concepts and Applications, Elsevier, Amsterdam, 1996.

[54] L.G. Wade. Organic Chemistry, sixth ed. Pearson Prentice Hall, New Jersey, 2006.

[55] H. Umeyama, K. Morokuma, Origin of alkyl substituent effect in the proton affinity of amines, alcohols, and ethers, J. Amer. Chem. Soc., 98 (15) (1976) 4400–4404.

[56] A. van der Vaart, K.M. Merz Jr, Charge transfer in small hydrogen bonded clusters, J. Chem. Phys., 116 (2002) 7380–7388.

[57] U. Koch, P.A. Popelier, Characterization of CHO hydrogen bonds on the basis of the charge density, J. Phys. Chem., 99 (1995) 9747–9754.

[58] P.A. Popelier, Characterization of a dihydrogen bond on the basis of the electron density, J. Phys. Chem., A 102 (1998) 1873–1878.

[59] P.A. Popelier, G. Logothetis, Characterization of an agostic bond on the basis of the electron density, J. Organomet. Chem., 555 (1998) 101–111.

[60] J.R. Lane, J. Contreras-García, J.P. Piquemal, B.J. Miller, H.G. Kjaergaard, Are bond critical points really critical for hydrogen bonding, J. Chem. Theory Comput., 9 (2013) 3263–3266.